Identification of Flow-Induced Noise Sources on Two-Dimensional High Lift Devices of Commuter Aircraft

Arifin Rasyadi Soemaryanto[1], M Fajar[2], TMI Hakim[3], Kurnia Hidayat[4], Sinung Tirtha[5]

[1,2,3,4,5]Aeronautics Technology Center, National Institute of Aeronautics and Space (LAPAN), Indonesia

[1]e-mail: arifin.rasyadi@lapan.go.id

Received: 07-12-2020. Accepted: 27-07-2021. Published: 30-12-2021

Abstract

On flight test development of commuter aircraft, it can be recognized that aircraft airframe noise is one of the problems that test pilot is concerned about when deploying aircraft's high-lift device into landing approach configuration. A numerical predictive tool of flow-induced noise generated by deployed high-lift devices of commuter aircraft is presented in this paper. The aircraft high-lift devices are consisting of vane and flap components. The aim of this study is to identify the sources of flow-induced noise on the wing and flap cross-section of the aircraft. This study investigates only two-dimensional effects and one configuration of flap deflection. Numerical computation is carried out using a CFD software with Large Eddy Simulation fluid turbulence model and Ffowcs-Williams & Hawkings analogy for acoustic prediction. Several sound receivers have been installed on the far-field and near-field region of the wing-vane-flap cross-section of aircraft to measure the sound spectra. It has been identified that the Cavity of the wing and vane-flap cross-section has the highest sound pressure level than another region. There is a vertical separation and shear layer which is contributed to the generation of sound emission downward the cross-section

Keywords: *computational aeroacoustics, computational aerodynamics, high-lift devices, aircraft design*

1. Introduction

Recently, on flight test development of commuter aircraft, it can be recognized that aircraft airframe noise is one of the problems that test pilot is concerned about when deploying aircraft high-lift devices during approach configuration. According to Perennes, for larger aircraft, airframe noise is a determinant source of flow-induced noise from aircraft, especially during the approach. In this scenario, airframe noise mainly originates from the high lift devices when fully deployed (Sophie Perennes, 1998). According to Molin, the flap can be considered as an isolated airfoil because there is a large slot that allowing communication between the under and an upper surface of the flap. Molin also has shown experimentally that a large part of flap noise is originating from the Cavity under the main wing (Molin, 2000). Molin has implemented the Amiet formulation (Amiet, 1975) with the aim of developing a complete high-lift noise prediction model on velocity disturbances in the slat cove and the flap cove. The results have been compared with flyover aircraft noise measurements made [Ma1] on Airbus A340. Brook et al. l, in their study, stated a flow-induced noise on isolated airfoil can be classified into three main generation mechanisms, turbulent boundary layer - trailing edge (TBL-TE) noise, laminar boundary layer - vortex shedding (LBL-VS) noise, and Separation Stall (S-S) noise (Brooks T.F., 1989). De Gennaro et al. l present the results of numerical experiments that capturing tonal airborne noise on the adopted test case of a NACA 0012 isolated airfoil (De Gennaro, Kuhnelt, & Zanon, 2017).

In this study, the aircraft's high-lift device consists of flap and vane-flap; it is a different configuration from other previous studies, as stated in the last paragraph. It is suspected the air that is flowing through the wing, vane, and flap components are generating a flow-induced noise around the region. Due to the difficulties in providing acoustics sensors in the commuter aircraft flight test development, a numerical predictive tool has been used to identify the source of flow-induced on the high-lift devices. The aim

of this study is to identify the sources of flow-induced noise on the wing and flap cross-section of the aircraft, with an expectation that the simulation solution can be validated later by external noise measurement on the wing and flap surface of the aircraft.

This article is investigated the flow-induced noise generated by high-lift devices in a two-dimensional wing configuration or constant cross-section only. The two-dimensional noise sources are continuously distributed along the span. Several simulation cases with a 2-dimensional cross-section of aircraft wingspan (**Figure 1**), a wing chord geometry of 2800 mm, and a flap chord of 600 mm have been simulated. The numerical simulation is carried out using commercial CFD software both for solving and post-processing the cases.

2. Methodology

2.1. Related Works

This section is presenting the related work, which has been a reference to choose the methods applied in this article, the two-dimensional Unsteady Large Eddy Simulation methodology as a turbulent model for aerodynamic simulation and coupled with the Ffwocs Williams and Hawkings (FW-H) for the acoustic prediction. The approach has been chosen because of the previous work of De Gennaro et al. 1, which is showing a low computational burden and capacity to predict the LBL-VS tonal noise. Due to the lack of availability of experimental sound-pressure data of the commuter aircraft high-lift devices, the verification is using data from the previous work done by Sahasranaman et al. 1 on airfoil NACA 0012 (Ashwin Sahasranaman, 2019).

2.2. Problem Definition

From the previous work on predicting airfoil or high-lift device noise, it is known that the sound is generated in the flow region and propagated through the far-field. Hybrid methods are introduced to decouple the flow generation from the acoustic propagation in the far-field, so consequently allowing the methods adopted for the various regions. One of the hybrid methods is Ffowcs-Williams & Hawkings (FW-H) analogy (Ffowcs Williams, 1969). FW-H is an extended work of Curle's analogy (Curle, 1955) by taking into account the sound generation from the arbitrary motion of a body in a turbulent flow. The governing of the FW-H equation is a generalization of Curle's analogy that the source terms of the equation are rewritten by taking account of boundary effects. The equation is essentially an inhomogeneous wave equation that can be derived by manipulating the continuity equation and the Navier-Stokes equation.

Turbulent flows are characterized by eddies with a wide range of length and time scales. Large Eddy Simulation (LES), therefore, falls between Direct Navier-Stokes (DNS) and Reynolds Averaging Navier-Stokes (RANS) in terms of the fraction of the resolved scales. In LES, momentum, mass, energy, and other passive scalars are transported mostly by large eddies and resolve directly. This study chose the Smagorinsky-Lilly model as turbulent viscosity and was first proposed by Smagorinsky (Smagoransky, 1963). In the Smagorinsky-Lilly model, the eddy-viscosity is modeled by,

$$\mu_t = \rho {L_s}^2 |\overline{S}| \tag{2-1}$$

where L_s is the mixing length for sub-grid scales?

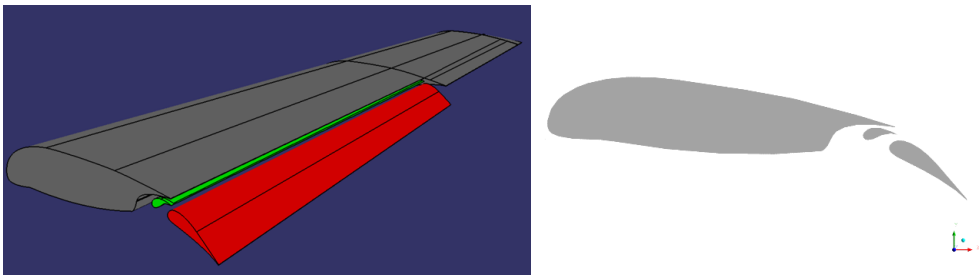

Figure 2-1. Wing and HLD Cross-Section of Commuter Aircraft

2.3. Method

The simulation flowchart describes the simulation process in Figure 2-2. The flow domain is solved using transient condition and unsteady LES turbulence model, resulting from an unsteady flow solution of the domain. The acoustics solution, in the form of sound pressure, is extracted using the FW-H analogy. The sound-pressure signals are processed to compute the frequency band and/or one-third octave band of the acoustic pressure sound spectra. To compute the sound spectra, the power spectral density (PSD) is calculated by applying the Discrete Fourier Transform (DFT) of the acoustic pressure signal from the simulation. For accelerating the computation, Fast Fourier Transform (FFT) routines are implemented. The Fourier transform express sound-pressure signals for a periodic set of N sampled points, (φ_k), as a finite trigonometric series:

$$\varphi_k = \sum_{n=0}^{N-1} \widehat{\varphi_k} e^{2\pi kn/N} \; ; \; k = 0,1,2,\ldots,(N-1) \tag{2-2}$$

and/or

$$\widehat{\varphi_n} = \frac{1}{N} \sum_{k=0}^{N-1} \widehat{\varphi_k} e^{-2\pi kn/N} \; ; \; n = 0,1,2,\ldots,(N-1) \tag{2-3}$$

which represents the n^{th} or k^{th} term in the Fourier transform of the signal.
To filtering the signal, the Hanning window is used with the formulation below,

$$W_j = \begin{cases} 0.54 - 0.46\cos\left(\dfrac{8\pi j}{N}\right) \text{ with } \dfrac{N}{8} < j \dfrac{7N}{8} \\ 1 \end{cases} \tag{2-4}$$

For the frequency band analysis, PSD is computed using the formula of,

$$PSD(f_n) = \frac{E(f_n)}{\Delta_f} \text{ with } n = 1,2,\ldots,N/2 \tag{2-5}$$

where Δ_f is the frequency step in the discrete spectrum, and the Fourier mode power $E(f_n)$ is computed as,

$$E(f_n) = \begin{cases} 0.5\left(2\left|\hat{\varphi}_n\right|\right)^2 & n = 0,1,2,\ldots,N/2-1 \\ \left|\hat{\varphi}_n\right|^2 & n = N/2 \end{cases} \tag{2-6}$$

For the one-third octave analysis, PSD is defined for the frequency band (f_{band}) as,

$$PSD(f_{band}) = \sum E(f_n) \tag{2-7}$$

where N includes all of the Fourier modes belonging to the band.

This article is presenting sound-spectra as decibel level using Sound Pressure Level (SPL) as a parameter. The formulation below is using to calculate the SPL of simulation results,

$$SPL = 10\left(\log \frac{PSD}{p_{ref}^{2}}\right) \tag{2-8}$$

where PSD is the power spectral density for either a particular frequency band and one-third octave band and p_{ref} is the reference acoustic pressure, with a value 2x10^{-5} Pa.

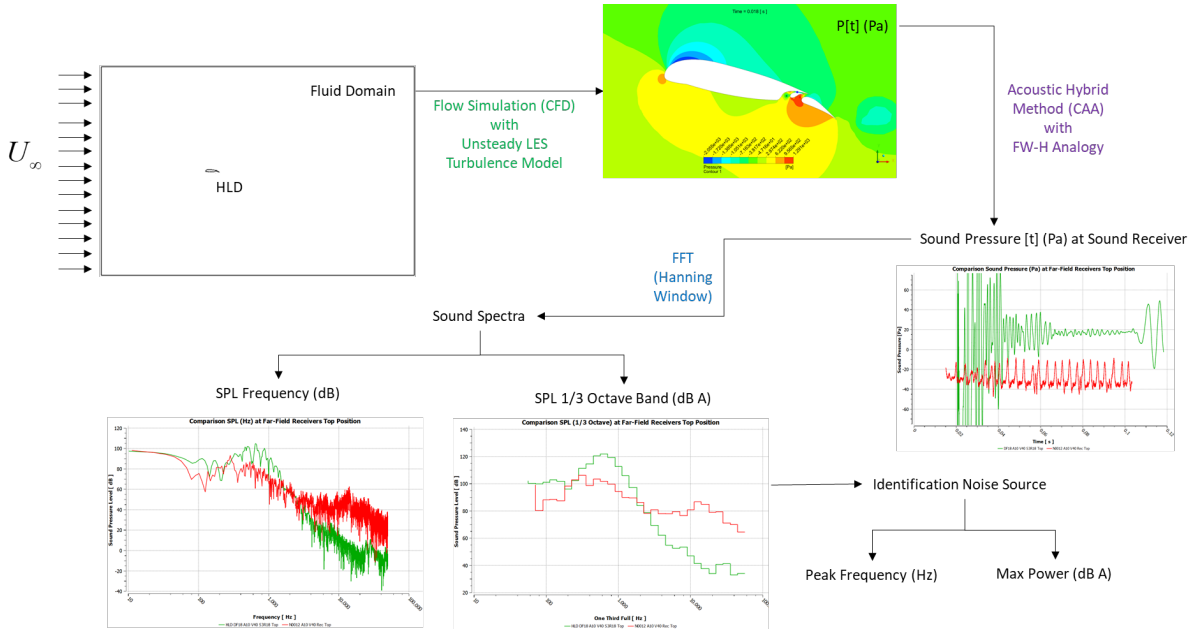

Figure 2-2. Simulation Flowchart

3. Result and Analysis

In this article, the flow-induced noise has been identified on one configuration of flap deflection, which is flap configuration on aircraft approach. The section below is presenting the simulation setting, results, and analysis of the simulation.

3.1. Simulation Setting

The mesh is generated to the geometry of the wing and high-lift devices component cross-section (see Figure 3-1). The wing and high-lift devices cross-section contain a two-dimensional airfoil with a total length of 2.15 m. The far-field of fluid domain is placed at a proper range from the leading and trailing edge of the airfoil cross-section, and a box-type structured grid is generated (see Figure 3-2). To ensure the boundary layer generation in the airfoil wall, the near-wall resolution of $y^+ < 1$ is generated. The simulations are performed at Re = 0.6 x 10^6 with an inlet velocity of 40 m/s, an angle of attack of 10 degrees, and a 30-degrees flap deflection for approach configuration. The airfoil cross-section is defined as a no-slip wall, and the pressure-outlet condition is used at the outlet boundary. The simulation is performed at the unsteady condition with flow-time from 0 to 1 second. A timestep of 2.5 x 10^{-5} is used for converting the time domain to a frequency domain of 0 to 12500 Hz. A non-iterative time advancement is chosen with the bounded second-order implicit transient formulation. The LES with Smagorinsky-Lilly turbulence model is solved with fractional step scheme and PRESTO pressure spatial discretization.

3.2. Simulation Results and Analysis

The aero-acoustics simulation has been conducted to identify the noise sources from near-field and far-field regions of a two-dimensional wing and high-lift devices of commuter aircraft. Several sound receivers have been placed over the components to obtain sound spectrum from the near-field and far-field region of the wing and high-lift devices cross-section. Covering near-field region from Cavity under the wing, wing trailing

edge, and flap trailing edge (see Figure 3-3) and the far-field region from the front, top, bottom, and back area of the components (see Figure 3-4).

Figure 3-5 and Figure 3-6 show the pressure fluctuation of approach configuration simulation cases on near-field and far-field regions. The microphones are receiving a pressure fluctuation that is generated from unsteady flow around components. The fluctuation is on the time domain; to convert it to the frequency domain, an FFT processing with Hanning window is used. So, the sound or noise signals at each receiver have been obtained in the form of a sound spectrum (see Figure 3-7 and Figure 3-8).

Due to the difficulties in providing acoustics sensors in the commuter aircraft flight test development, the simulation model cannot be validated. Thus, the simulation model can be verified. The verification of the simulation model is conducted by comparing sound spectrum results with benchmark data of NACA 0012 airfoil done by (Sahasranaman et al. l; 2019). One of the far-field receivers on Top area of the domain has been compared (see Figure 3-9).

To identify the main noise sources from near-field and far-field regions of the two-dimensional wing and high-lift devices of commuter aircraft, these are identified on the term of the peak frequency and maximum power of each receiver. In the near-field region, several receivers at cavities under the wing and also receivers at the wing trailing edge and flap trailing edge have been compared. It has been identified that the main noise source of the near-field region is coming from Cavity no two receivers. The location of the receiver is under the wing and on top of the vane component. Figure 3-10 shows the peak frequency around 600 Hz, and the maximum power of 130 dB A is coming from that receiver. On the other area in the far-field region, it has been identified that the main noise source is coming from Top area receivers. The receiver shows the peak frequency around 500 Hz and the maximum power of 77 dB A of its spectrum (see Figure 3-11).

From the analysis of sound level pressure result at all receivers and also the flow visualization, it has been identified that main flow-induced noise sources are coming from a recirculating flow at the Cavity under the wing that making a flow separation through a small gap area between the main wing and vane component which has a high pressure (see Figure. 3-12). So, the highest noise level comes from the area between the main wing and vane. The flow visualization of the solution also has been compared with a work done by (Molin, 2000).

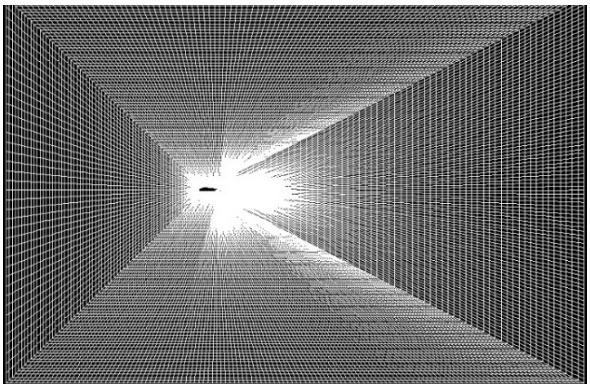

Figure 3-1. Simulation mesh on the near-field region of the wing and high-lift devices cross-section with 30-degree deflection

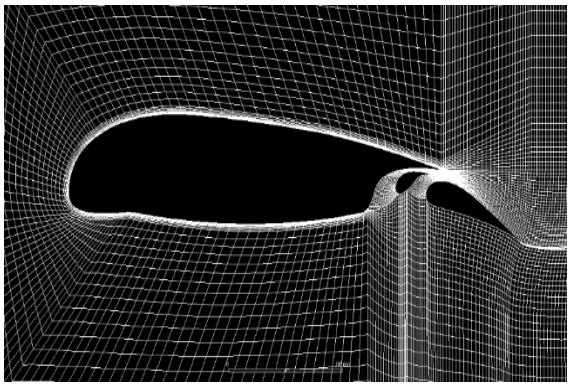

Figure 3-2. Simulation mesh on the far-field region of the wing and high-lift devices cross-section with 30-degree deflection

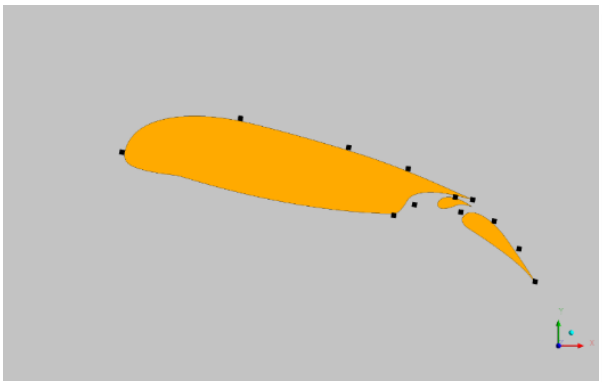

Figure 3-3. Position of Sound Receivers at Near-field Area. Three receivers cover cavities area underwing and vane. Two receivers cover TE Wing and TE Flap. Others receivers cover other areas distributed chordwise.

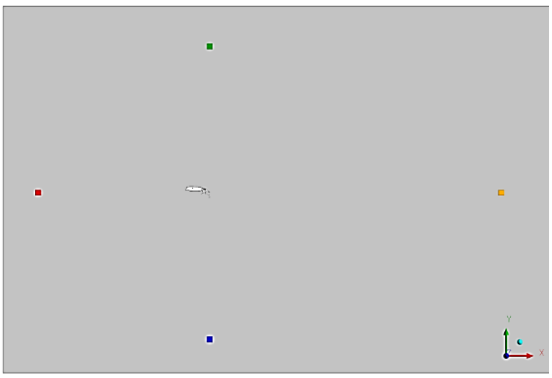

Figure 3-4. Position of Sound Receivers at Far-field Area. Distance from LE to Front Area is 12 m (Red); from TE to Top & Bottom Area is 12 m (Green & Blue); from TE to Back Area is 26 m (Orange)

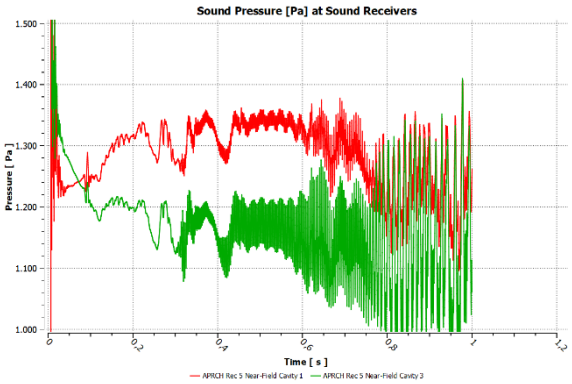

Figure 3-5. Pressure Fluctuation on Near-field Sound Receivers of Cavities Area of Wing-HLD Cross Section

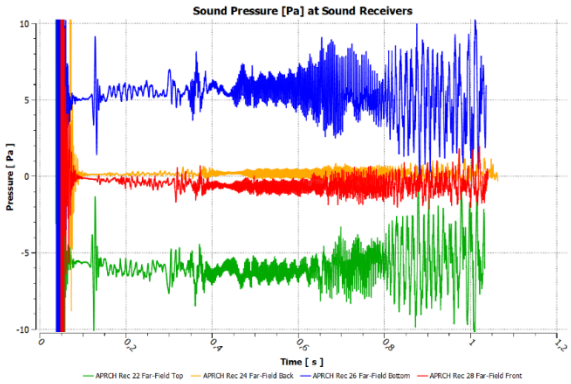

Figure 3-6. Pressure Fluctuation on Far-field Sound Receivers of Top, Back, Bottom, and Back Area of Fluid Domain

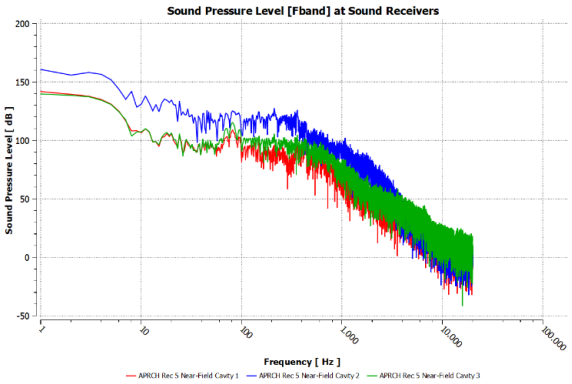

Figure 3-7. Sound Spectrum (SPL scale) of Near-field Sound Receivers of Cavities Area Under the Wing

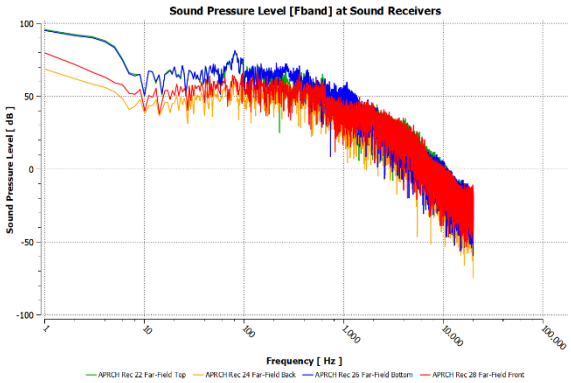

Figure 3-8. Sound Spectrum (SPL scale) of Far-field Sound Receivers of Top, Back, Bottom, and Back Area of Fluid Domain

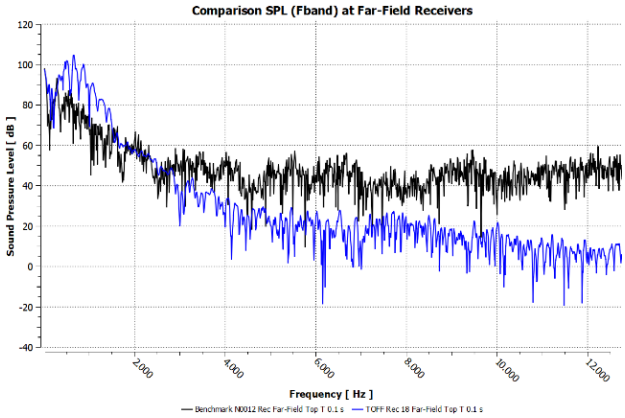

Figure 3-9. Comparison of Sound Spectrum (SPL scale) on Far-field Sound Receivers (Top) of Simulation Case & NACA 0012 Benchmark Data (Sahasranaman et al. l; 2019)

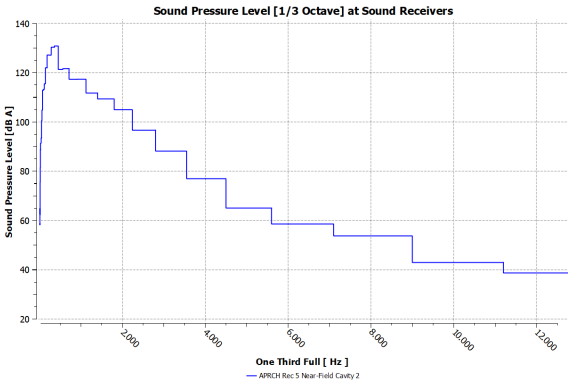

Figure 3-10. Sound Spectrum (SPL scale 1/3 octave band) of Identified Receiver with highest noise source on the near-field area. We identified maximum power of 130 dB A and identified a peak frequency around 600 Hz.

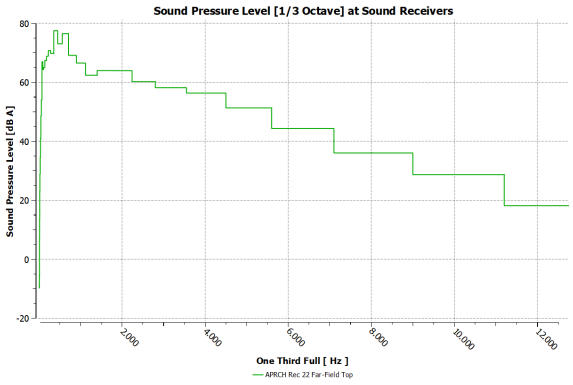

Figure 3-11. Sound Spectrum (SPL scale 1/3 octave band) of Identified Receiver with highest noise source on the far-field area. Identified maximum power of 77 dB A identified peak frequency around 500 Hz

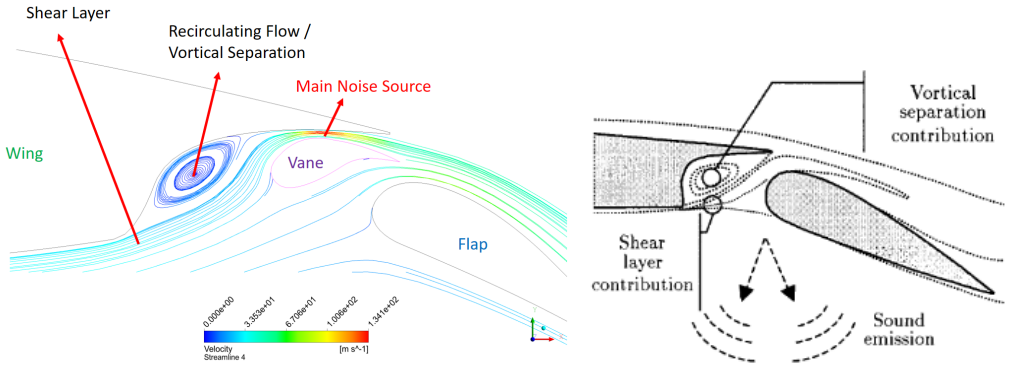

Figure 3-12. Flow visualization (velocity streamline) on cavities area under the wing and top of vane component indicating a contribution to generating a main flow-induced noise source compared to Molin`s simulation (Molin:2000).

4. Conclusions

Numerical computation is carried out using a CFD software with Large Eddy Simulation fluid turbulence model and Ffowcs-Williams & Hawkings analogy for acoustic prediction. Several sound receivers or microphones have been installed on the far-field and near-field region of the wing-vane-flap cross-section of aircraft to measure the sound spectra. It has been identified that the Cavity of the wing and vane-flap cross-section has the highest sound pressure level than another region by comparing sound level pressure magnitude and also the visualization of the flow. There is a vertical separation and shear layer which is contributed to the generation of sound emission downward the cross-section. According to regulation, if that noise source is propagated to the far-field region, it is still below the allowed level. On the other hand, for the passenger comfortability in the cabin area of the aircraft, the noise level should be under consideration to be reduced.

Acknowledgments

This research and development are a part of the development of N219 aircraft funded by PUSTEKBANG. We would like to thank PTDI for providing the data research and manuscript writing and also to Mr. Agus Aribowo as Head of PTN programe.

Contributorship Statement

All of the authors are the main contributor. ARS developed the simulation and prepared the manuscript; MF analyzed the results and prepared the manuscript; TMIH developed the simulation and analyzed the results; STP prepared the manuscript; KH prepared the manuscript.

References

Amiet, R. (1975). Acoustic radiation from an airfoil in a turbulence stream. *Journal of Sound and Vibration, Vol 41, No 4*, 407 - 420.

ANSYS-Fluent 14.5 Theory Guide. (2012). ANSYS Inc.

Ashwin Sahasranaman, S. S. (2019). Computational Aeroacoustic Characteristics of an Airfoil at Higher Reynolds Number. *AIP Conference Proceedings 2161.*

Brooks T.F., P. D. (1989). Aero-foil self-noise and prediction. *NASA Reference Publication 1218.*

Curle, N. (1955). The influence of solid boundaries upon aerodynamic sound. *Proceedings of the Royal Society of London. Series A Mathematical and Physical Sciences, 231(1187)*, 505-514.

De Gennaro, M., Kuhnelt, H., & Zanon, A. (2017). Numerical Prediction of the Tonal Airborne Noise for a NACA 0012 Aerofoil at Moderate Reynolds Number Using a Transitional URANS Approach. *PAN Archives of Acoustics Vol. 42, No. 4*, 653-675.

Ffowcs Williams, J. E. (1969). Sound generation by turbulence and surfaces in arbitrary motion". *Philosophical Transactions of Royal Society of London Vol 342*, 264-321.

Molin, N. (2000). The Use of Amiet's Methods In Predicting The Noise From 2D High-Lift Devices. *AIAA.*

Smagoransky, J. (1963). General Circulation Experiments With the Primitive Equations. I. The Basic Experiment. *Month Wea*, 99-164.

Sophie Perennes, M. R. (1998). Aerodynamic Noise Of A Two-Dimensional Wing With High-Lift Devices. *AIAA.*

Takuji Kurotaki, e. a. (2008). Numerical simulation around NACA0015 with tonal noise generation. *46th AIAA Aerospace Sciences Meeting and Exhibit.* AIAA.

Wang, M. (2005). Computation of trailing-edge aeroacoustics with vortex shedding. In *Center for Turbulence Research Annual Briefs* (pp. 379 - 388).